The Astrophysical Journal Letters, 856:L14 (8pp), 2018 March 20 https://doi.org/10.3847/2041-8213/aab54f

Young Surface of Pluto's Sputnik Planitia Caused by Viscous Relaxation

Qiang Wei[1], Yongyun Hu[1], Yonggang Liu[1], Douglas N. C. Lin[2], Jun Yang[1], and Adam P. Showman[1]
[1] Laboratory for Climate and Atmosphere—Ocean Studies, Department of Atmospheric and Oceanic Sciences, School of Physics, Peking University, Beijing, 100871, People's Republic of China; ygliu@pku.edu.cn
[2] Department of Astronomy and Astrophysics, University of California at Santa Cruz, CA 95064, USA
Received 2018 January 22; revised 2018 February 25; accepted 2018 March 7; published 2018 March 23

Abstract

One of the most prominent features of Pluto observed by the New Horizon mission is the absence of craters on Sputnik Planitia (SP). Vigorous thermal convection could renew the SP surface with sufficient depth at a timescale of ∼500,000 years. Here we present numerical simulations demonstrating that craters can be removed much more quickly across all of SP by viscous relaxation of nitrogen (N_2) ice. The timescale of relaxation is in years if the N_2 layer is 4 km thick and the viscosity is as determined in the lab, and will increase to 10^4 years if the viscosity is 10^4 times larger than the measured value. For such high viscosity, the thermal convection will have a timescale of greater than 10^6 years if it happens at all, so that the relaxation timescale is still more than 2 orders of magnitude shorter. The relaxation timescale decreases with increasing thickness and temperature of the ice layer. The existence of pits on SP can be explained by the surface enhancement of viscosity. Such enhancement does not have significant influence on the relaxation timescale of craters with diameters greater than a few kilometers. Therefore, although convection is required to explain the polygon shapes, it may have a lesser role in the absence of craters on SP. The viscous relaxation mechanism can readily explain the nondetection of both craters and polygon shapes on the southeast SP.

Key words: convection – Kuiper Belt objects: individual (Pluto) – methods: numerical – planets and satellites: composition – planets and satellites: physical evolution – planets and satellites: surfaces

1. Introduction

The lack of impact craters on the predominantly N_2 ice sheet of Sputnik Planitia (SP) indicates efficient resurfacing processes (Robbins et al. 2016). It has been suggested that the crater retention age is no more than ∼10 million years (Stern et al. 2015b; Trilling 2016). Recent simulation studies indicate that vigorous thermal convections of N_2 ice can remove craters within a million or 500,000 years, assuming that the thickness is a few kilometers to several tens of kilometers (McKinnon et al. 2016; Trowbridge et al. 2016). While thermal convection offers an explanation to the observed polygon shapes on the SP ice sheet, there could be other resurfacing processes that contribute to the absence of craters and the young surface. Lack of craters on the southern Lightly Pitted Plains or Deeply Pitted Plains (White et al. 2017), where the thickness of the N_2 ice sheet may not be enough to initiate convection (McKinnon et al. 2016; Umurhan et al. 2017), calls especially for an alternative mechanism.

In previous literature, viscous relaxation has been applied to interpreting observed craters on icy moons, such as Europa (Thomas & Schubert 1986, 1987), Ganymede (Dombard & McKinnon 2000; Bland et al. 2017), Enceladus (Passey 1983; Bland et al. 2012), and Iapetus (Robuchon et al. 2011). A rough estimate using the scaling method was also given prior to New Horizon's encounter to Pluto (Stern et al. 2015a). However, the constraint by thermal convection on the thickness of the ice layer on SP was not available to them yet, so the scaling relation they have used was based on the thick-ice limit (crater diameters $\ll$ ice thickness). Moreover, the timescale of relaxation they obtained based on the scaling relation for Newtonian rheology, compared to that obtained from the detailed calculation using nonlinear rheology presented herein, substantially overestimates (by 3 orders of magnitude) its dependence on temperature. Therefore, a quantitative estimate of the timescale of viscous relaxation of craters on the N_2 ice layer of SP is warranted. Results from numerical simulations demonstrate that viscous relaxation of N_2 ice is a more efficient process in resurfacing the SP ice sheet, and that the timescale of crater removal is 3 orders of magnitude shorter than that of thermal convections.

2. Method

The numerical model used here is the Ice Sheet System Model (ISSM) version 4.11 (Larour et al. 2012), which was originally developed for studying water glaciers on Earth and recently adapted for the study of CO_2 glacial flow of Martian south polar layered deposits (Smith et al. 2016). The full Stokes equation is solved to simulate crater relaxations herein. We modify the original model with Pluto's gravity of 0.62 m s^{-2} (Stern et al. 2015b) and N_2 ice density of 0.98 g cm^{-3} (Scott 1976; Satorre et al. 2008). Non-Newtonian creep parameters (see Equation (1)) are taken from laboratory measurements at 45 K and 56 K (Yamashita et al. 2010), the same as those adopted in studies of convection (McKinnon et al. 2016; Trowbridge et al. 2016) and glacier flows (Umurhan et al. 2017).

$$\dot{\varepsilon} = A\sigma^n. \tag{1}$$

We follow the method of Moore et al. (2016) and linearly extrapolate n down to the surface temperature on SP, which yields $n = 1.9915$ at 38 K (Grundy et al. 2016; Umurhan et al. 2017). It has been tested that a value of 2.2, as used in convection studies (e.g., McKinnon et al. 2016), will increase the timescale of viscous relaxation by less than 50%, which is negligible compared to the influence of many other factors. We also accept the assumption in the same work that the prefactor

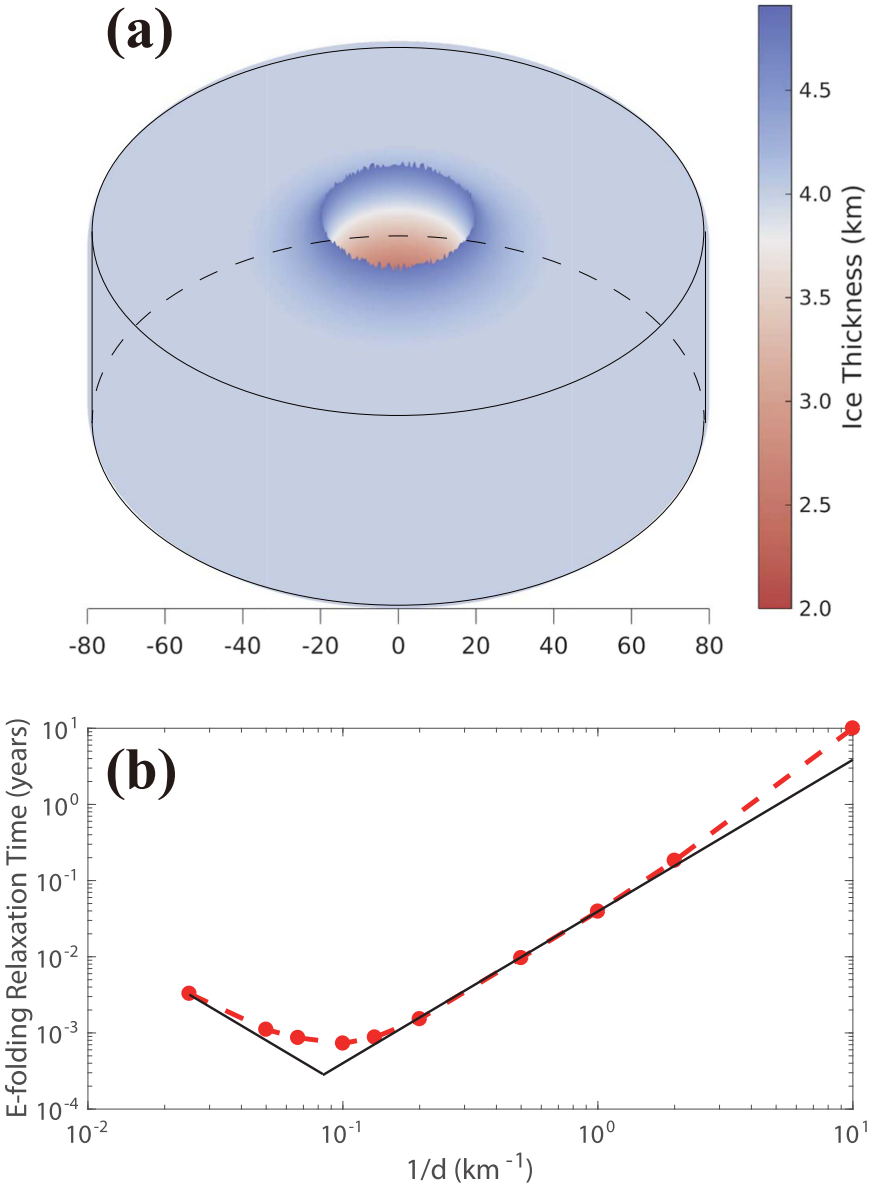

Figure 1. (a) Model initialization and (b) e-folding relaxation times as an inverse function of crater diameter d. The model domain is initialized with a cylinder of N_2 ice and a crater at the center of the cylinder. Here, the crater has an apparent depth of 2 km and a diameter of 40 km, and the corresponding ice cylinder has a diameter of 160 km. The max height of the crater rim is 0.75 km. In all of the simulations in (b), the aspect ratio of crater depth and diameter is set to 1 : 10, N_2 ice thickness is 4 km, and ice temperature is 38 K. The solid black lines illustrate the scaling relationships of Equations (3) and (4) respectively. The red dashed–dotted curve indicates numerical results.

is an Arrhenius type with the following form:

$$A(T) = A(45\ \mathrm{K}) \exp\left(\frac{T_A}{45\ \mathrm{K}} - \frac{T_A}{T}\right), \tag{2}$$

where $A(45\ \mathrm{K}) = 0.005\ \mathrm{MPa}^{-\mathrm{n(T)}}\ \mathrm{s}^{-1}$ and T_A is determined to be 422 K by plugging in the corresponding numbers for $T = 56$ K. The prefactor A at 38 K is 0.00089 $\mathrm{MPa}^{-\mathrm{n}}\ \mathrm{s}^{-1}$, as determined by Equation (2). Due to large uncertainties in the viscosity of N_2 ice, we have also tested cases where effective viscosity is increased by 4 orders of magnitude ($\sim 10^{14}$ Pa s) and cases where effective viscosity at the surface is further increased by another 4 orders of magnitude ($\sim 10^{18}$ Pa s) and linearly recovered to the interior values ($\sim 10^{14}$ Pa s) within 100 or 200 m.

Forget et al. (2017) concluded through climate modeling, that the net change rate of surface N_2 ice thickness in 2015 due to condensation and sublimation was 4.6×10^{-3} m and -1.33×10^{-2} m per Earth year at 7.5 °N and 45 °N, respectively. Both processes should have no significant influence on N_2 ice thickness during its orbital period. Consequently, the surface mass balance is set to zero. In most simulations, the ice cylinder has a uniform temperature of 38 K and homogenous viscosity. Because viscosity decreases with temperature, such an assumption yields an upper limit of crater retention ages compared to one with increasing temperature toward the bottom.

In all simulations, the model domain is cylindrical and its diameter is always four times that of the crater rim-to-rim diameter (Figure 1(a)). To assist the comparison of the results among different cases and relate to analytic results, we assume a simple crater shape in all plotted experiments, the cavity of which conforms to a fourth-order polynomial (Dombard & McKinnon 2006). It produces little difference in relaxation timescale compared to complex craters (Zahnle et al. 2003; Bray & Schenk 2015; Moore et al. 2015 see Section 3.1 for details). For simplicity, the ejecta blanket is represented with a fourth-order power law as well, and the average height of a jagged (due to limited spatial resolution; Figure 1(a)) crater rim is about 25% of the total crater depth in all simulations. The ejecta blanket, represented with third-order laws, was also tested, showing minimal difference in the result. The depth of the crater varies widely due to substrate composition, impact viscosity, and angle. Without prior knowledge, we adopt an apparent depth (difference between the bottom of the crater and the background ice surface; all depths are apparent depths unless otherwise specified) of 2 km for craters with a diameter of 40 km as a midpoint from studies of icy satellites (Schenk 1989) and carry out sensitivity tests ranging from 0.5 km to 4 km.

The model domain is meshed horizontally with triangles at a size of $1/50$ of the crater diameter and divided vertically into 10–30 layers depending on the length scale on which topography varies. Every layer contains ~6400 vertices. Further increasing resolution produces no significant difference in the results (<5%). The sides of the domain are free-slip in the vertical direction and fixed in the horizontal, and all velocities are forced to zero at the bottom boundary. Allowing basal slip with friction coefficient similar to that of Earth's ice-sheet decreases retention age by approximately 10%–30% in thin-ice (crater diameter $\gg$ ice thickness) cases.

A benchmark experiment was first conducted to simulate a slab of N_2 ice flowing down a surface of constant slope. The results were very close to previous analytical solutions (Moore et al. 2016). Crater relaxation experiments were conducted with assumed Newtonian rheology, and with crater diameters both greater and smaller than the thickness of the ice layer. The relaxation timescales were accordant with those deducted by scaling analysis (e.g., Thomas & Schubert 1986). For non-Newtonian rheology, the scaling between an e-folding relaxation timescale and viscosity parameters and crater parameters can be easily derived for both the thin-ice limit,

$$\tau_{\rm thin} \sim \frac{1}{A}\frac{d^{n+1}}{H^{n+2}\triangle h^{n-1}(\rho g)^n} \quad (3)$$

and the thick-ice limit,

$$\tau_{\rm thick} \sim \frac{\triangle h}{A(\rho g \triangle h)^n d}, \quad (4)$$

where H is the thickness of the N_2 ice layer, d and $\triangle h$ are the diameter and apparent depth of craters, respectively, ρ is the density of N_2 ice on SP, and g is the surface gravity on Pluto. When the creep exponent $n = 1$, the scaling relations recover those for the Newtonian rheology (Haskell 1935; Jeffreys 1952; Scott 1967; Thomas & Schubert 1986). Compared to the scaling for Newtonian rheology, the most important change in Equations (3) and (4) is probably the appearance of $\triangle h$, which is a consequence of the dependence of effective viscosity on stress for non-Newtonian rheology. Clearly, as $\triangle h$ decreases during the relaxation of a crater, the relaxation timescale increases, making the timescales above less useful than those for Newtonian rheology. However, instantaneous relaxation timescales for non-Newtonian rheology are sometimes still estimated with numerical models (e.g., Dombard & McKinnon 2000). They may be compared to those obtained by the scaling analysis above for some sort of model validation. As shown in Figure 1(b), they compare relatively well. Moreover, the relationship between the instantaneous relaxation timescale and horizontal wavelength shown in Figure 1(b) is qualitatively similar to that for the Newtonian case (e.g., Figure 1 of Parmentier & Head 1981 note that d on the x-axis of Figure 1(b) is crater diameter, so $1/d$ is only approximate to wavenumbers even after the multiplication of a factor π). For such a scaling relationship, updoming is expected to be seen near the center of the crater as it relaxes in the thick-ice region. This is indeed seen in our model simulations. All of these factors provide confidence in the model being used for simulating crater relaxation on N_2 ice. We investigate the dependence of crater relaxation timescales on temperature, crater depth, N_2 ice thickness, and crater diameter, etc., using this model.

3. Crater Retention Age for Different N_2 Ice Viscosity

3.1. Viscosity from Measurement

In this section, the N_2 ice viscosity is assumed to be that experimentally measured by Yamashita et al. (2010), which has been used in previous convection studies (McKinnon et al. 2016; Trowbridge et al. 2016). Figure 2 shows simulated crater shapes and N_2 ice flows at different stages of viscous relaxation. Here, the crater is initially 2 km in apparent depth and 40 km in diameter, and the thickness of the N_2 ice sheet is 4 km. Comparison of Figures 2(a) and (b) indicates that the crater shape experiences rapid changes at the very early stage of viscous relaxation due to large stress and non-Newtonian rheology. The slope of the crater wall becomes flat through time (Figure 2(c)). Ice flows (arrows) are driven by pressure gradient force, and horizontal velocities are generally greater, underlying regions with greater surface slopes (Greve & Blatter 2009). The spatial variation of horizontal velocities is such that divergence and convergence of ice mass fluxes occur beneath the rim and the crater bottom, respectively. As a result, vertical motions are induced by mass continuity, which tends to lower the rim and lift the center. At the same time, the walls move toward the center. These processes reduce the topographic differences, i.e., remove the crater. The ice velocity decreases rapidly with time. The maximum velocity is about 5.5×10^6 m per Earth year ($\rm yr^{-1}$; unless otherwise specified, Earth year is always meant by "year" hereafter) at the beginning (Figure 2(a)), more than two orders of magnitude larger than the largest velocity of modern glaciers on Earth. However, ice velocity quickly drops to 2.1×10^3 m $\rm yr^{-1}$ after one month (Figure 2(c)), and to 7.3×10^1 m $\rm yr^{-1}$ after one year (Figure 2(d)). This crater relaxes almost entirely in the thin-ice limit, i.e., short wavelength features relax faster than

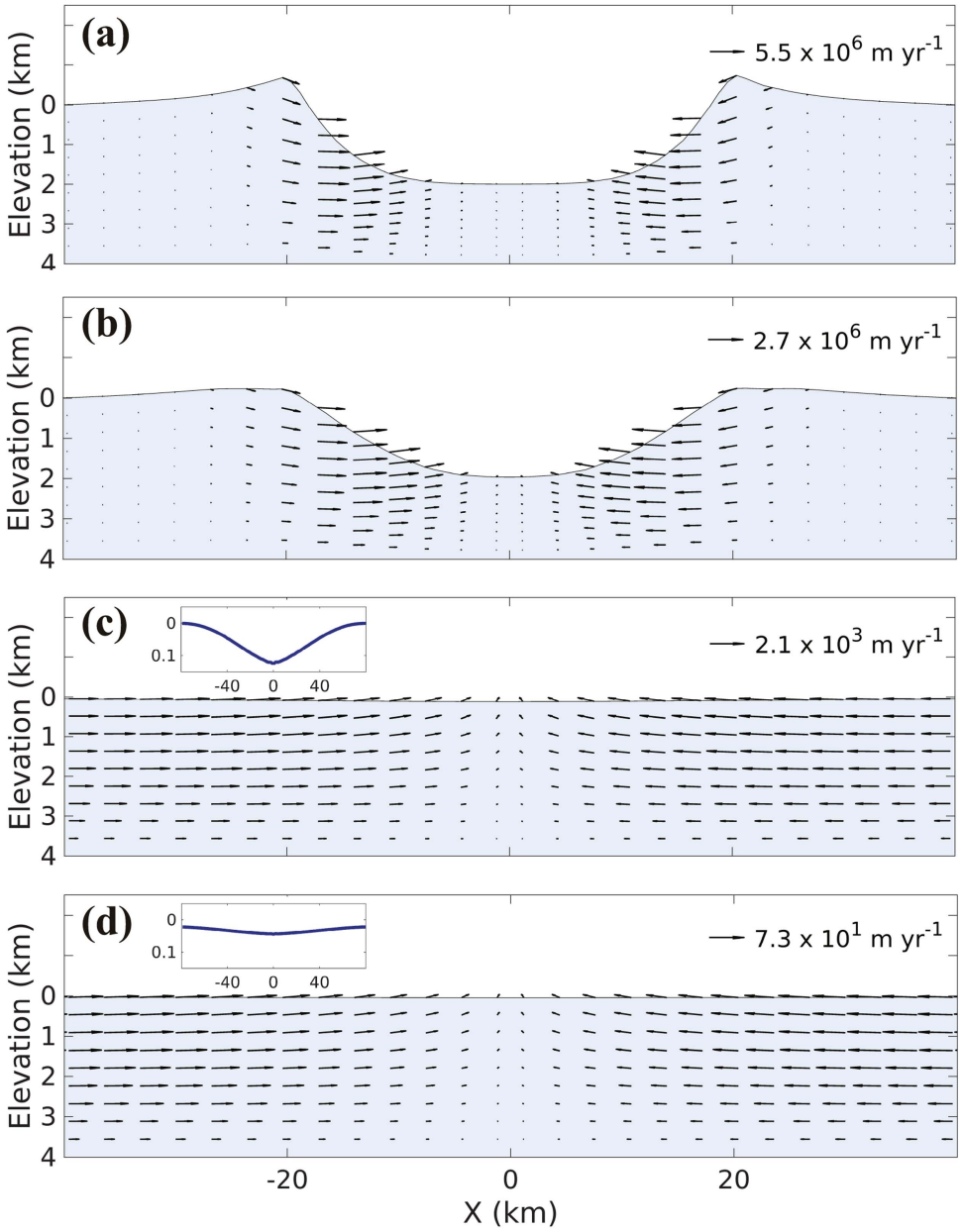

Figure 2. Vertical cross-sections of a crater at different relaxation stages. The crater is initially 2 km in depth, 40 km in diameter, and the surface temperature is 38 K. Arrows represent N_2 ice velocities. The length scale of the maximum N_2 ice velocity is marked in the upper-right corner. (a) At the initial time; (b) within an Earth day; (c) after one month; and (d) after one year. In plots (c) and (d), the insets zoom in with greater vertical exaggeration.

the long wavelength features (Figure 1(b)) so that the rim relaxes faster than the crater cavity (Figure 2(b)).

We first test the dependence of viscous relaxation timescales to ice temperatures, as shown in Figure 3(a). We define the crater retention age as the relaxation time when the depth of a crater becomes as shallow as 25 m. Such a conservative choice is at least 5 times smaller than the current limit of stereogrammetry and by all means ensures a nondetection through photoclinometry. At 38 K, it takes about 0.8 years for a crater with an initial depth of 2 km on a 4-km-thick ice sheet to relax to a depth of 25 m (Figure 3(a)). The viscosity of N_2 ice decreases with increasing temperatures (Yamashita et al. 2010). Our simulations yield retention ages of 0.5, 0.3, and 0.2 years for temperatures of 42, 46, and 50 K, respectively. The crater retention ages obtained here are about 5 orders of magnitude shorter than convective overturn timescales (McKinnon et al. 2016; Trowbridge et al. 2016). This low sensitivity with temperature implies that the vertical temperature gradient induced by Pluto's geothermal heat flux (Robuchon & Nimmo 2011) would have a small influence on crater retention age. Further simulations show that the retention age will reduce by approximately 50%–100% if a temperature gradient of 5 K/km is considered (McKinnon et al. 2016; Nimmo et al. 2016).

N_2 ice has a phase transition between α and β phases at 35.6 K (Fray & Schmitt 2009). It was reported that for a stress of 88.2 kPa N_2 ice is in the cubic α-phase at 35.5 K and in the hexagonal β-phase at and above 37.9 K, and that N_2 ice in the α-phase creeps approximately five times slower than in the β-phase (Alekseeva & Strzhemechny 2012). The results here

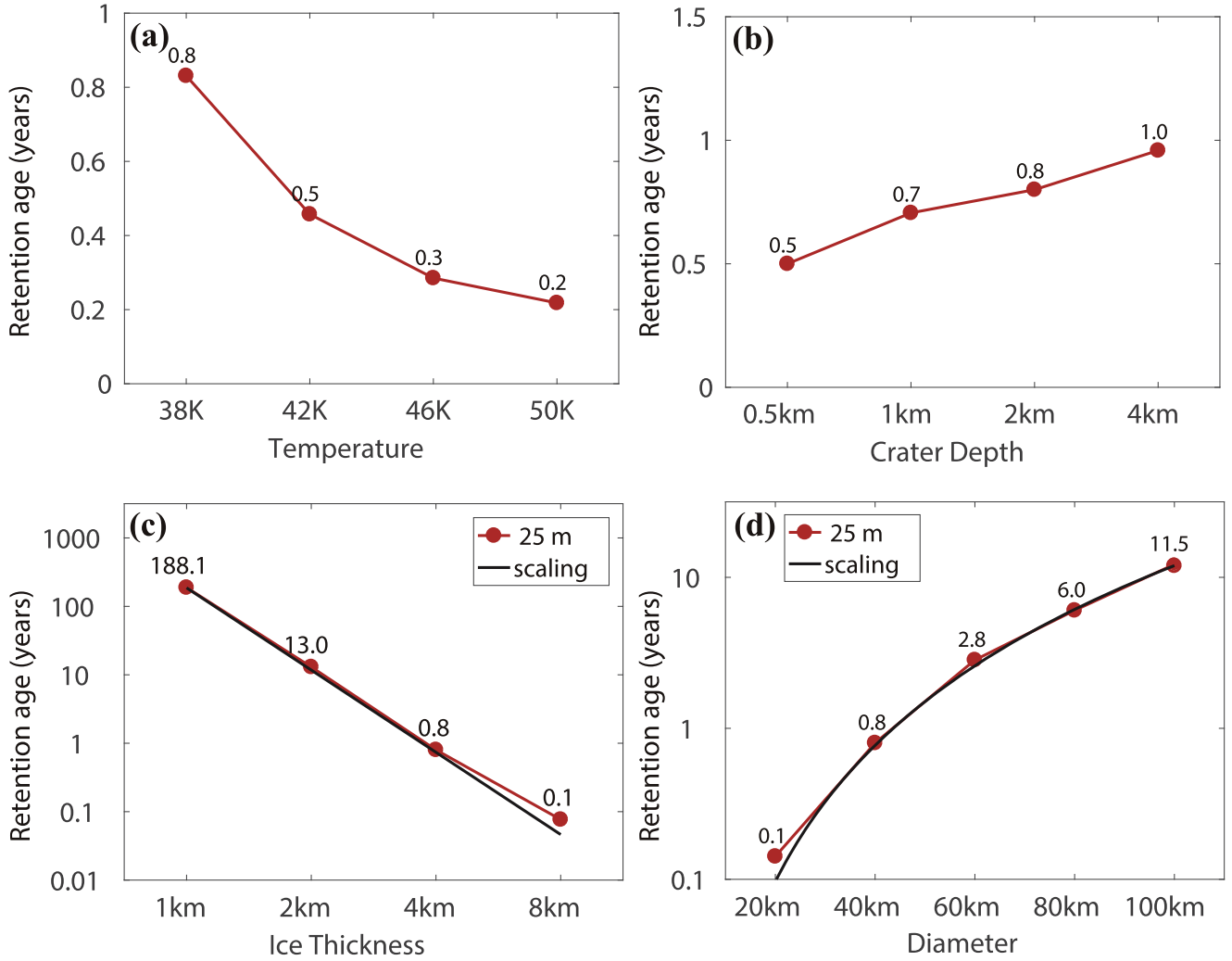

Figure 3. Crater relaxation times with (a) different temperatures, (b) crater depth, (c) N_2 ice thickness, and (d) crater diameters. The benchmark case is 38 K with a crater that is initially 2 km deep, 40 km in diameter on 4 km thick ice. Each test shown in (a)–(d) varies by one parameter. The red dots and lines represent the timescale for the crater to relax to a depth of 25 m. The black curves are the relaxation times estimated from scaling analysis for $\tau_{\rm thin}$, i.e., Equations (3) and (4) in Section 2, and fitted to the numerical result.

suggest that the short crater retention ages calculated here are robust against the uncertainty and variations of surface temperature, which may arise from atmospheric conditions, surface albedo, and orbital effects (Earle et al. 2017).

Figure 3(b) indicates that the crater retention age increases only modestly with crater depth. For a crater with a depth of 0.5 km, its retention age is 0.5 years. As the depth increases to 4 km, the crater retention age increases to 1.0 year. The results in Figure 3 suggest that the crater retention age is insensitive to crater depth as long as the crater depth is shallower than ice thickness.

Figure 3(c) demonstrates that the crater retention age is very sensitive to N_2 ice thickness. For N_2 ice thickness of 1 km, the retention age is about 188 years for a crater with 40 km diameter and 2 km depth. We assumed in this case that the surrounding N_2 ice relaxes into the crater that penetrates to the water ice substrate. A thin (0.1m) layer of N_2 was artificially placed on the exposed water ice to avoid modification of the no-slip boundary condition. As N_2 ice thickness is increased to 2 km, the crater retention age drops to 13 years. For N_2 ice thickness of 4 and 8 km, the retention ages rapidly drop to 0.8 and 0.1 years, respectively. It appears that each doubling N_2 ice thickness leads to a decrease of crater retention ages by a factor of about 15. The scaling relation in Equation (3) gives a value of 16, so it may be justified for more general use in a rough estimate of how crater retention age scales with relevant parameters for non-Newtonian rheology.

For N_2 ice thickness of 4 km, the minimum instantaneous e-folding relaxation timescale occurs when the crater diameter is $\sim$10 km (Figure 1(b)). This indicates that for any sizable craters on SP, their retention age increases with diameters, contrary to the scaling analyses adopted in some previous rough estimates since they assumed a thick-ice layer (Stern et al. 2015a; Trilling 2016). For a simple crater of diameter 20 km, the retention age is 0.1 year (Figure 3(d)). As crater diameter increases to 40 and 80 km, the retention ages are extended to 0.8 and 6.0 years, respectively. Each doubling of crater diameter leads to an increase in crater retention ages by a factor of 8. This is also consistent with the scaling relation in Equation (3), which yields an eight times increase in relaxation time for each doubling of crater diameters for $n = 2$. Additional tests show that the 100 km diameter complex craters with a central peak, pit, or peak-ring (Bray & Schenk 2015) exhibit retention ages of 11.9, 12.0, and

Table 1
Relaxation Timescale against Thickness of Enhanced Viscosity Layer

Type	Diameter	Depth	Thickness of Enhanced Viscosity ($10^8\times$) Layer[a]	e-folding Relaxation Timescale (years)	Retention Age (years)
Pit	0.3 km	0.1 km	0 m	2.26×10^3	$>4.23 \times 10^{3b}$
			100 m	2.45×10^6	$>5.61 \times 10^{6b}$
			200 m	7.26×10^6	$>1.58 \times 10^{7b}$
	1 km	0.2 km	0 m	2.86×10^2	$>1.26 \times 10^{3b}$
			100 m	1.51×10^3	$>1.83 \times 10^{5b}$
			200 m	7.31×10^4	$>5.96 \times 10^{5b}$
Crater	40 km	2 km	0 m	3.70×10^1	8.96×10^3
			100 m	5.70×10^1	1.30×10^4
			200 m	5.73×10^1	1.31×10^4

Note.
[a] Ice beneath this layer has $10^4\times$ the experimental viscosity (Yamashita et al. 2010).
[b] These numbers are the time it takes for the pits to relax to a depth of 25 m, while their retention age is defined by 4 m.

11.6 years, respectively, almost the same as that of 11.5 years for a simple crater of the same depth. The decrease in the depth-diameter ratio commonly observed on large, complex craters has little influence on the retention age, as was described for simple craters above where changes in depth result in little alteration to retention time.

For pits that have horizontal scales of ~10–1000 meters (Howard et al. 2017; Moore et al. 2017; White et al. 2017), Figure 1(b) indicates that their retention age increases with decreasing diameters. This allows expansion in the initial formation stage due to sublimation (Buhler & Ingersoll 2018; Moore et al. 2017). Simulated with a rimless sinusoidal shape, a retention age of 0.8 years is obtained for a 1 km wide pit (the maximum depth is fixed at 200 m for 1 km wide pits and 100 m for pits of all other diameters, in rough agreement with maximum depth of North-Central SP pits). Here we choose the retention age of a pit as the relaxation time when the maximum depth decreases to 4 m, since the vertical resolution of photoclinometry may be higher for smaller horizontal scale. As the diameter is reduced to 0.3 km and 0.1 km, the retention age is increased to 1.6 and 43 years, respectively. These are likely too small to explain their pervasive existence on SP.

3.2. Enhanced Viscosity

The retention age of craters scales linearly with viscosity. For example, if the viscosity is increased uniformly by 4 orders of magnitude (i.e., A in Equation (1) is reduced by the same magnitude), the retention age of a crater with 40 km diameter and 2 km apparent depth increases from ~0.8 years to ~9000 years, also 4 orders of magnitude (Table 1). If the surface of the ice layer is stiffened by another 4 orders of magnitude, and it recovers linearly with depth to the interior value in 100 m or 200 m, it has little effect on the retention age of the crater above. However, it has dramatic influence on the retention age of a pit. For a medium sized pit of 300 m diameter and 100 m depth (Buhler & Ingersoll 2018), the e-folding relaxation timescale increases from ~2000 years to 10^7 years (Table 1). For a large pit of 1 km diameter, the e-folding relaxation timescale increases from ~300 years to 1500 years and 10^5 years for surface layer thickness of 100 m and 200 m, respectively. The 25 m retention ages are much larger than the e-folding relaxation timescale and are not precisely calculated in some cases due to long computing time (Table 1). The surface enhanced viscosity does significantly influence the relaxation of the rim of a relatively small crater. For a 4 km diameter crater with an apparent depth of 500 m, using the same enhanced viscosity ($10^8\times$ experimental value at the surface and $10^4\times$ in the interior), it takes approximately 10,000 years for the rim height to relax from 125 m to 50 m, a difference that would escape detection with stereogrammetry due to limited vertical resolution (Schenk et al. 2017) and photoclinometry due to solar angle (Buhler & Ingersoll 2018).

4. Discussion

The SP ice sheet consists of a small amount of CH_4 and CO ice, in addition to the major constituent of N_2 ice (Grundy et al. 2016; Protopapa et al. 2017; Schmitt et al. 2017). Although the viscosity of CO ice has not been measured under the Pluto condition, it was suspected to be similar to the viscosity of N_2 ice due to similar molecular bond structure (Moore et al. 2016; Umurhan et al. 2017). CH_4 ice is likely much more viscous due to higher melting temperature (Eluszkiewicz & Stevenson 1990; Yamashita et al. 2010), and may increase the viscosity of the N_2:CH_4:CO ice layer. Due to unknown rheology of the mixed state, we carry out a simulation for pure CH_4 ice as an upper limit for higher ice viscosity. Same extrapolation methods were used on the experimental CH_4 rheological data, yielding $A = 8.84 \times 10^{-6}\,\mathrm{MPa}^{-n}\,\mathrm{s}^{-1}$ and $n = 1.97$. It is found that the retention ages of craters on a CH_4 ice layer of 4 km thick is 2 to 3 orders of magnitude longer than those on the N_2 ice, e.g., 326 years versus 0.8 years for a crater with 40 km diameter and 2 km depth. Such retention age is still 2 orders of magnitude shorter than that of thermal convection.

The viscosity of the near surface ice on SP may be much higher than that at depth. First, grain size at the surface could grow through sintering to the observed value of 59 cm (Protopapa et al. 2017) and result in higher viscosity due to grain size sensitive creep with $p = 1.4 \sim 3$ (Goldsby & Kohlstedt 2001; Durham et al. 2010). The grain beneath the surface is balanced at smaller sizes by more active dynamic recrystallization under high stresses (Poirier 1985; Durham et al. 2010). Second, potentially higher concentrations of CH_4 and CO due to sublimation of N_2, along with deposition of impurities hinted by distinctly dark materials on the pit floor in some cases (Moore et al. 2017), could also act as a binding agent that increases the ice's viscosity. Third, it might even be possible that the surface of N_2 ice falls into a different creep

regime. Relaxation of topography samples subsurface mechanical properties over a depth comparable to the wavelength (Parmentier & Head 1981). Therefore, the high surface viscosity entails slow relaxation of a pit that complies to the rate required by pit growth through sublimation (Buhler & Ingersoll 2018), yet it has a much smaller influence on the relaxation of large craters (diameters greater than ~10 km).

If the viscosity of the interior N_2 ice on SP is 4 orders of magnitude higher than the values measured in the lab (Yamashita et al. 2010), the mean velocity of convection will decrease to the subcentimeter range. Solving Equations (7) to (12) of Trowbridge et al. (2016) using parameters given in the same paper, gives $\overline{v_{\rm conv}} = 1.5\ {\rm cm\ yr^{-1}}$ with the measured viscosity and $\overline{v_{\rm conv}}' = 0.3\ {\rm cm\ yr^{-1}}$ with 10^4 times the measured viscosity. The latter value is significantly smaller than the lower limit ($\sim 1.5\ {\rm cm\ yr^{-1}}$) of the surface velocity inferred from pit sublimation rates (Buhler & Ingersoll 2018). The slower convective velocity also implies that the timescale of crater removal by convection is extended by half an order of magnitude. Meanwhile, at such high viscosity, the Rayleigh number calculated through Equation (1) in McKinnon et al. (2016) will be approximately 1000, very close to the critical Rayleigh number for sluggish lid convection, which is also ~1000, as given by Equation (3)) of the same paper. Consequently, the viscosity of the ice layer on SP cannot be much larger than 10^4 times the measured value if convection is to be used to explain the polygon shape there. Even for interior viscosity of 10^4 times the measured value, the crater retention age of 10^4 years obtained here is still at least 2 orders of magnitude shorter than that of the convective timescale.

5. Conclusions

Our simulations have demonstrated that viscous relaxation is a very efficient process to remove craters on N_2 ice sheets. If the ice layer on SP is composed of pure N_2 ice that is 4 km thick and its viscosity is the same as that measured in the lab by Yamashita et al. (2010), the crater retention age against viscous relaxation is on the order of years to 10 years, 5 orders of magnitude shorter than the timescale at which convection removes craters. If the viscosity of the ice is 4 orders of magnitude larger than the measured value due to the grain-size effect, mixing with a large amount of CH_4 ice or other unknown factors, the retention age increases to 10^4 years. For such viscosity, the timescale of crater removal due to convection may increase from 10^6 to $\sim 5 \times 10^6$ years, which is still more than 2 orders of magnitude longer than that due to viscous relaxation. Further increase of viscosity of the ice layer may not be supported if thermal convection is to be used to explain the polygon shapes on SP. If the softening of deep ice is considered as a result of temperature increase at depth, the timescale of relaxation will be even shorter, by about a factor of 2, for large craters.

Existence of pits on the surface of SP may be explained by significant increase of viscosity near the surface of the ice layer. If the surface viscosity is 10^8 times larger than the measured value and linearly decreases by 4 orders of magnitude within the upper 100 m, a pit with 300 m diameter and 100 m depth will have a relaxation timescale of 10^6 years. Such a timescale is long enough to maintain their existence or even expand under the influence of sublimation. More importantly, such near surface enhancement of viscosity does not have any significant influence on the relaxation timescales of craters with diameters on the order of 10 km. Therefore, we propose that the absence of craters on SP is most likely due to viscous relaxation of the craters rather than due to resurfacing by thermal convection, but the latter is still necessary to explain the polygon shapes on SP. This relaxation mechanism could be especially important for the southeast region of SP where neither craters nor the convection cell were observed.

We thank Dave J. Stevenson and Kelsi Singer for helpful discussions that greatly improved our understanding on certain topics. We also thank the anonymous referee for a thorough and critical review of an earlier version of this paper. Y.H. and Q.W. are supported by the National Natural Science Foundation of China under grants 41761144072 and 41530423.

Author Contributions

Y.H. and D.N.C.L. proposed the research. Y.H., Y.L., and Q.W. designed the numerical experiments. Q.W. and Y.L. performed the simulations. A.S. and Y.L. performed the scaling analysis. All authors contributed to analyzing simulation results and the writing of the paper.

The authors declare no competing financial interests.

Correspondence and requests for materials should be addressed to Y.L. (ygliu@pku.edu.cn).

ORCID iDs

Qiang Wei https://orcid.org/0000-0001-5625-477X
Yongyun Hu https://orcid.org/0000-0002-4003-4630
Yonggang Liu https://orcid.org/0000-0001-8844-2185
Douglas N. C. Lin https://orcid.org/0000-0001-5466-4628
Jun Yang https://orcid.org/0000-0001-6031-2485

References

Alekseeva, L. A., & Strzhemechny, M. A. 2012, LTP, 38, 534
Bland, M. T., Singer, K. N., McKinnon, W. B., & Schenk, P. M. 2012, GeoRL, 39, L17204
Bland, M. T., Singer, K. N., McKinnon, W. B., & Schenk, P. M. 2017, Icar, 296, 275
Bray, V. J., & Schenk, P. M. 2015, Icar, 246, 156
Buhler, P. B., & Ingersoll, A. P. 2018, Icar, 300, 327
Dombard, A. J., & McKinnon, W. B. 2000, GeoRL, 27, 3663
Dombard, A. J., & McKinnon, W. B. 2006, JGRE, 111, E01001
Durham, W., Prieto-Ballesteros, O., Goldsby, D., & Kargel, J. 2010, SSRv, 153, 273
Earle, A. M., Binzel, R. P., Young, L. A., et al. 2017, Icar, 287, 37
Eluszkiewicz, J., & Stevenson, D. J. 1990, GeoRL, 17, 1753
Forget, F., Bertrand, T., Vangvichith, M., et al. 2017, Icar, 287, 54
Fray, N., & Schmitt, B. 2009, P&SS, 57, 2053
Goldsby, D. L., & Kohlstedt, D. L. 2001, JGRB, 106, 11017
Greve, R., & Blatter, H. 2009, Dynamics of Ice Sheets and Glaciers (Berlin: Springer)
Grundy, W., Binzel, R. P., Buratti, B. J., et al. 2016, Sci, 351, aad9189
Haskell, N. 1935, Phy, 6, 265
Howard, A. D., Moore, J. M., White, O. L., et al. 2017, Icar, 293, 218
Jeffreys, H. 1952, RSPSA, 214, 281
Larour, E., Seroussi, H., Morlighem, M., & Rignot, E. 2012, JGRF, 117, F01022
McKinnon, W. B., Nimmo, F., Wong, T., et al. 2016, Natur, 534, 82
Moore, J. M., Howard, A. D., Schenk, P. M., et al. 2015, Icar, 246, 65
Moore, J. M., Howard, A. D., Umurhan, O. M., et al. 2017, Icar, 287, 320

Moore, J. M., McKinnon, W. B., Spencer, J. R., et al. 2016, Sci, 351, 1284
Nimmo, F., Hamilton, D. P., McKinnon, W. B., et al. 2016, Natur, 540, 94
Parmentier, E., & Head, J. 1981, Icar, 47, 100
Passey, Q. R. 1983, Icar, 53, 105
Poirier, J.-P. 1985, Creep of crystals: High-temperature Deformation Processes in Metals, Ceramics and Minerals (Cambridge: Cambridge Univ. Press)
Protopapa, S., Grundy, W. M., Reuter, D. C., et al. 2017, Icar, 287, 218
Robbins, S. J., Singer, K. N., Bray, V. J., et al. 2016, Icar, 287, 187
Robuchon, G., & Nimmo, F. 2011, Icar, 216, 426
Robuchon, G., Nimmo, F., Roberts, J., & Kirchoff, M. 2011, Icar, 214, 82
Satorre, M. Á., Domingo, M., Millán, C., et al. 2008, P&SS, 56, 1748
Schenk, P. M. 1989, JGRB, 94, 3813
Schenk, P. M., Beyer, R. A., McKinnon, W. B., et al. 2017, AGU Fall Meeting, Abstract P24C-08
Schmitt, B., Philippe, S., Grundy, W. M., et al. 2017, Icar, 287, 229
Scott, R. F. 1967, Icar, 7, 139
Scott, T. A. 1976, PhR, 27, 89
Smith, I., Larour, E., Putzig, N., Greve, R., & Schlegel, N. 2016, LPICo, 1926, 6072
Stern, S. A., Bagenal, F., Ennico, K., et al. 2015b, Sci, 350, aad1815
Stern, S. A., Porter, S., & Zangari, A. 2015a, Icar, 250, 287
Thomas, P. J., & Schubert, G. 1986, JGRB, 91, 453
Thomas, P. J., & Schubert, G. 1987, JGRB, 92, 749
Trilling, D. E. 2016, PLoSO, 11, e0147386
Trowbridge, A., Melosh, H., Steckloff, J., & Freed, A. 2016, Natur, 534, 79
Umurhan, O. M., Howard, A. D., Moore, J. M., et al. 2017, Icar, 287, 301
White, O. L., Moore, J. M., McKinnon, W. B., et al. 2017, Icar, 287, 261
Yamashita, Y., Kato, M., & Arakawa, M. 2010, Icar, 207, 972
Zahnle, K., Schenk, P., Levison, H., & Dones, L. 2003, Icar, 163, 263